molecules

MDPI

Article

A New Tetradentate Mixed Aza-Thioether Macrocycle and Its Complexation Behavior towards Fe(II), Ni(II) and Cu(II) Ions

Sze-Wing Ng [1,2,†], Siu-Chung Chan [1,†], Chi-Fung Yeung [1,2], Shek-Man Yiu [1] and Chun-Yuen Wong [1,2,*]

1 Department of Chemistry, City University of Hong Kong, Tat Chee Avenue, Kowloon, Hong Kong
2 State Key Laboratory of Terahertz and Millimeter Waves, City University of Hong Kong, Tat Chee Avenue, Kowloon, Hong Kong
* Correspondence: acywong@cityu.edu.hk; Tel.: +852-3442-6831
† These authors contributed equally to this work.

Academic Editors: Emilia Furia and Tiziana Marino
Received: 5 April 2020; Accepted: 22 April 2020; Published: 27 April 2020

Abstract: A new tetradentate mixed aza-thioether macrocyclic ligand 2,6-dithia[7](2,9)-1,10-phenanthrolinophane ([13]ane(phenN_2)S_2) was successfully synthesized. Reacting metal precursors [Fe(CH_3CN)$_2$(OTf)$_2$], Ni(ClO_4)$_2$·6H_2O, and Cu(ClO_4)$_2$·6H_2O with one equivalent of [13]ane(phenN_2)S_2 afforded [Fe([13]ane(phenN_2)S_2)(OTf)$_2$] (**1**), [Ni([13]ane(phenN_2)S_2)](ClO_4)$_2$ (**2**(ClO_4)$_2$), and [Cu([13]ane(phenN_2)S_2)(OH_2)](ClO_4)$_2$ (**3**(ClO_4)$_2$), respectively. The structures of [13]ane(phenN_2)S_2 and all of its metal complexes were investigated by X-ray crystallography. The [13]ane(phenN_2)S_2 was found to behave as a tetradentate ligand via its donor atoms N and S.

Keywords: first-row transition metal ion; macrocyclic ligand; coordination complex

1. Introduction

Coordination chemistry of first-row transition metal ions has attracted considerable attention for decades due to their high biological relevance. Not only do the coordination complexes serve as models to study biologically related metallomolecules, but they also provide insights into biomimetic designs [1–15]. Among a reservoir of ligand designs, macrocycles have been demonstrated to be a valuable type of auxiliary ligand for these studies because (1) many macrocycles are incorporated in naturally-occurring metalloproteins and metalloenzymes, such as porphyrin in haemoglobin and corrin in vitamin B_{12}, and (2) the properties of the derived metal complexes can be modulated via modification in the ring size and donor atoms on the macrocyclic ligands.

Our group has recently initiated a paradigm in scrutinizing the reactivity between low-valent transition metal precursors and heteroatom-functionalized alkynes [16–29]. Gratifyingly, several Ru- and Os-heterocyclic complexes reported by our group exhibit interesting biological applications. The success of preparing these functional metalated heterocyclic complexes prompted us to expand the scope of our studies to other biologically relevant first-row transition metals. Moreover, we envision that employing multidentate macrocycles as auxiliary ligands in these studies can reduce the ambiguity in mechanistic elucidations because well-designed macrocycles can effectively minimize partial ligand dissociation. With these considerations in mind, we would like to prepare some new first-row transition metal complexes supported by macrocycles for analogous reactivity studies. Among a variety of macrocycles, we are interested in mixed phenanthroline-thioether ligands, not only because their preparation is straightforward but they are well-known to stabilize various low-valent first-row transition metal ions (Scheme 1) [30–47]. While most of the reported mixed phenanthroline-thioether

macrocycles are a 15-membered ring with 5 donor atoms to behave as pentadentate ligands, analogs with smaller ring sizes that can increase their conformational rigidity are rare. In this context, we report the preparation and complexation ability of a new tetradentate macrocyclic ligand 2,6-dithia [7](2,9)-1,10-phenanthrolinophane (denoted as [13]ane(phenN_2)S_2). To our delight, this macrocycle allows the preparation of low-valent transition metal complexes [Fe([13]ane(phenN_2)S_2)(OTf)$_2$], [Ni([13]ane(phenN_2)S_2)](ClO_4)$_2$ and [Cu([13]ane(phenN_2)S_2)(OH_2)](ClO_4)$_2$ under mild reaction conditions with high yields. The solid-state structures of [13]ane(phenN_2)S_2 and its metal complexes have been determined by X-ray crystallography. The success of preparing these macrocyclic complexes undoubtedly paves the way for performing further reactivity studies.

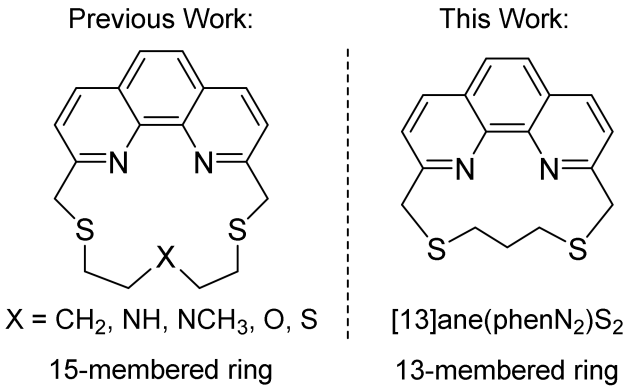

Scheme 1. Mixed phenanthroline-thioether macrocycles reported in previous works and this work.

2. Results and Discussion

2.1. Synthesis and Characterization of [13]ane(phenN_2)S_2

The new mixed aza-thioether macrocyclic ligand [13]ane(phenN_2)S_2 was prepared from cyclization between 2,9-bis(chloromethyl)-1,10-phenanthroline and 1,3-propanedithiol in the presence of Cs_2CO_3 as a base and source of template cation under high dilution conditions (Scheme 2). The 2,9-bis(chloromethyl)-1,10-phenanthroline can be synthesized in accordance with previously reported literature methods from 2,9-dimethyl-1,l0-phenanthroline as depicted in Scheme 2 [48–52]. The formation of this air-stable macrocycle was characterized by mass spectroscopy together with ^{1}H and ^{13}C-NMR spectroscopy.

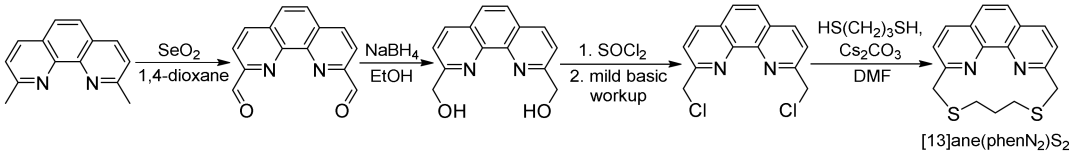

Scheme 2. Synthesis of [13]ane(phenN_2)S_2.

The structure of [13]ane(phenN_2)S_2 was further confirmed by X-ray crystallography (Figure 1). While the phenanthroline moiety of this macrocycle is essentially planar, the 13-membered ring adopts a folded conformation in the solid state. More specifically, the dimethylphenanthroline moiety is essentially planar whereas the -S(CH_2)$_3$S- chain is tilted over the phenanthroline unit, with an angle of 51.6° between the mean planes constructed by C(1), C(10), C(13), C(17) and C(13), C(17), S(1), S(2). The C-C bonds along the -S(CH_2)$_3$S- unit take on *anti* conformations. All the C-S bond distances (1.822(2)-1.823(2) Å) are typical for thioethers [47]. Since the lone pairs of the S-donors adopt exodentate orientation pointing out of the ring cavity, large conformational change is expected for [13]ane(phenN_2)S_2 to act as a tetradentate ligand via donor atoms N and S.

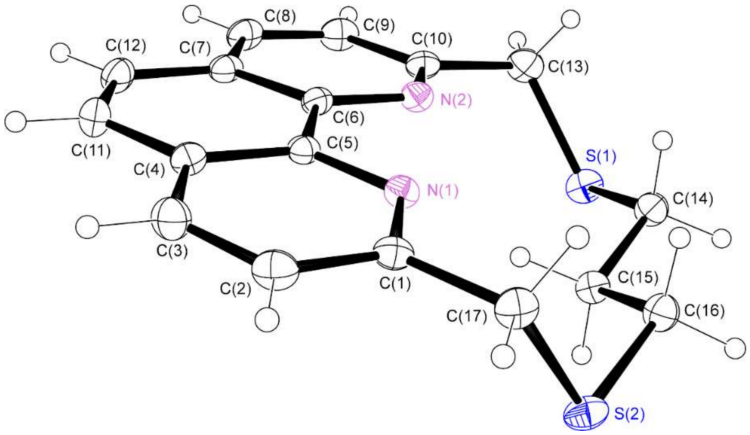

Figure 1. Perspective view of [13]ane(phenN_2)S_2 as represented by 30% probability ellipsoids. Selected bond lengths (Å) and angles (°): N(1)-C(1), 1.326(2); N(1)-C(5), 1.352(2); C(5)-C(6), 1.456(2); N(2)-C(6), 1.349(3); N(2)-C(10), 1.323(2); C(1)-C(17), 1.498(3); C(10)-C(13), 1.501(3); S(1)-C(13), 1.822(2); S(1)-C(14), 1.823(2); S(2)-C(16), 1.819(2); S(2)-C(17), 1.822(2); C(1)-C(17)-S(2), 114.6(1), C(10)-C(13)-S(1), 115.3(1); C(13)-S(1)-C(14), 103.5(1); C(16)-S(2)-C(17), 103.8(1).

To explore the possible low-energy conformers, the X-ray structure for [13]ane(phenN_2)S_2 was optimized at the density functional theory (DFT) level to yield the first conformer, Conformer **I**. The search for other low-energy conformers was then performed by exploring the torsional energy surface of the aliphatic chain, followed by structural optimization. Two other conformers, denoted as Conformers **II** and **III**, were obtained throughout the conformer search. These conformers **I**–**III** are labeled in ascending order of their relative energy (0.0, 1.2 and 4.4 kcal mol^{-1}, respectively). Their structures are depicted in Figure 2, with selected bond lengths (Å) and angles (°) summarized in Table 1. Notably, the structure of Conformer **I** is in good agreement with the X-ray structure, in which the two S atoms are tilted over the dimethylphenanthroline moiety in the same direction and the two C-C bonds on the -S(CH_2)$_3$S- unit take on *anti* conformation. On the other hand, one of the S atoms in Conformer **II** is coplanar with the dimethylphenanthroline moiety, while another S atom keeps tilting over the phenanthroline unit. Although the two S atoms in Conformer **III** are tilted over the dimethylphenanthroline moiety in the same direction, the C-C bonds on the -S(CH_2)$_3$S- unit take on a combination of *anti* and *gauche* conformations, making it structurally distinct from Conformer **I**. As none of these conformers have their donor atoms pointing to a common center, large distortion is expected for the ligand to act as a tetradentate ligand.

Table 1. Selected bond lengths (Å) and angles (°) for Conformers **I**–**III**.

Conformers	I	II	III
N(1)-C(1)	1.332	1.332	1.331
N(1)-C(5)	1.349	1.348	1.348
N(2)-C(6)	1.349	1.353	1.343
N(2)-C(10)	1.332	1.327	1.330
C(1)-C(17)	1.511	1.506	1.512
C(10)-C(13)	1.511	1.522	1.511
S(1)-C(13)	1.844	1.825	1.850
S(1)-C(14)	1.845	1.850	1.846
S(2)-C(16)	1.846	1.838	1.851
S(2)-C(17)	1.846	1.851	1.856
C(1)-C(17)-S(2)	114.5	112.9	111.6
C(10)-C(13)-S(1)	114.4	116.9	111.9
C(13)-S(1)-C(14)	102.7	101.7	101.8
C(16)-S(2)-C(17)	102.6	103.6	105.1

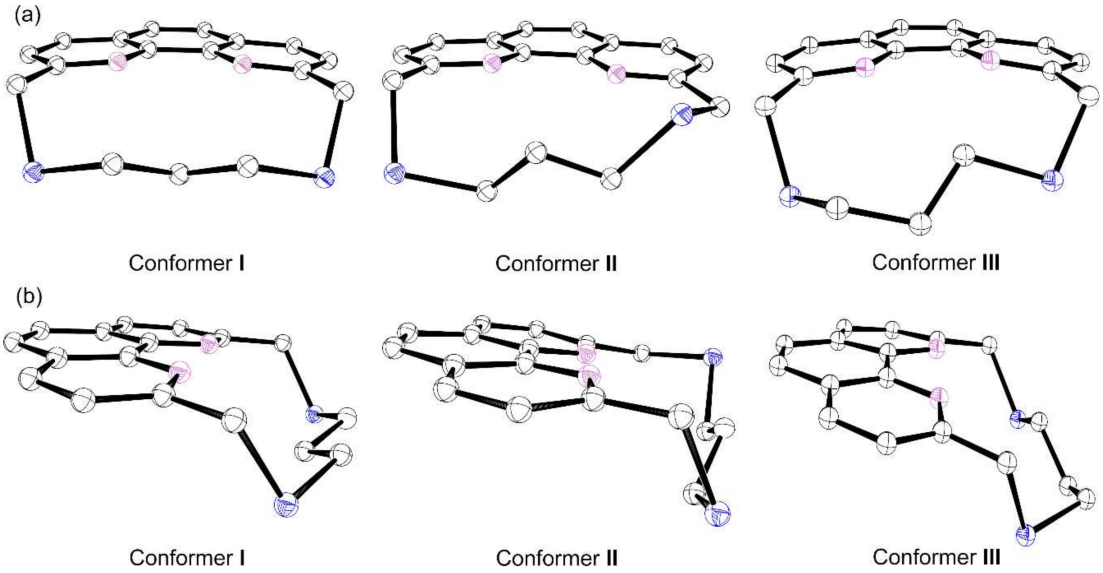

Figure 2. (**a**) Front views and (**b**) side views of three possible low-energy conformers of [13]ane($phenN_2$)S_2.

2.2. Synthesis and Characterization of [13]ane($phenN_2$)S_2-Containing Transition Metal Complexes

The coordination behavior of [13]ane($phenN_2$)S_2 ligand was explored with various first-row transition metal ions including Fe(II), Ni(II) and Cu(II) (Scheme 3). Reacting metal precursors [$Fe(CH_3CN)_2(OTf)_2$], $Ni(ClO_4)_2{\cdot}6H_2O$, and $Cu(ClO_4)_2{\cdot}6H_2O$ with one equivalent of [13]ane($phenN_2$)S_2 afforded a six-coordinated Fe complex [Fe([13]ane($phenN_2$)S_2)$(OTf)_2$] (**1**), four-coordinated Ni complex [Ni([13]ane($phenN_2$)S_2)]$(ClO_4)_2$ (**2**$(ClO_4)_2$), and five-coordinated Cu complex [Cu([13]ane($phenN_2$)S_2)(OH_2)]$(ClO_4)_2$ (**3**$(ClO_4)_2$), respectively. All of them are isolable in good yields (70–80%). It is noteworthy that both **2**$(ClO_4)_2$ and **3**$(ClO_4)_2$ are very stable in CH_3CN as their X-ray structures can be obtained upon recrystallization under ambient conditions. On the other hand, **1** exhibits a certain degree of instability towards air- and moisture-sensitive conditions. For example, the color of **1** changed from yellow to deep brown during recrystallization in CH_3CN under ambient conditions, leading to an ill-defined product. Despite this observation, **1** cannot be regarded as very air-sensitive since its UV-visible absorption profile in non-degassed CH_3CN remained unchanged for 16 h (Figure S1). The solubility of all metal complexes was also investigated in common organic solvents (CH_3CN, acetone, CH_2Cl_2, THF and MeOH) and H_2O. All of the three complexes were found to be soluble in CH_3CN. In addition, **1** is soluble in acetone and CH_2Cl_2, whereas **2**$(ClO_4)_2$ and **3**$(ClO_4)_2$ are soluble in H_2O. The solution magnetic moments for these complexes were determined via ^{1}H-NMR spectroscopy using the Evans method [53,54]; the Fe(II) and Ni(II) complexes were determined to possess high-spin electronic states (S = 2 for Fe and S = 1 for Ni), whereas the electronic spin determined for the Cu(II) complex was the expected S = 1/2. The molecular structures for all these metal complexes were determined by X-ray crystallography. Their perspective views and selected structural parameters are depicted in Figure 3, Figures 5 and 6. It is evident that [13]ane($phenN_2$)S_2 possesses structural flexibility to behave as a tetradentate ligand, and the energy required for the conformational change is expected to be small as complexes **1**, **2**$(ClO_4)_2$ and **3**$(ClO_4)_2$ can be prepared at room temperature.

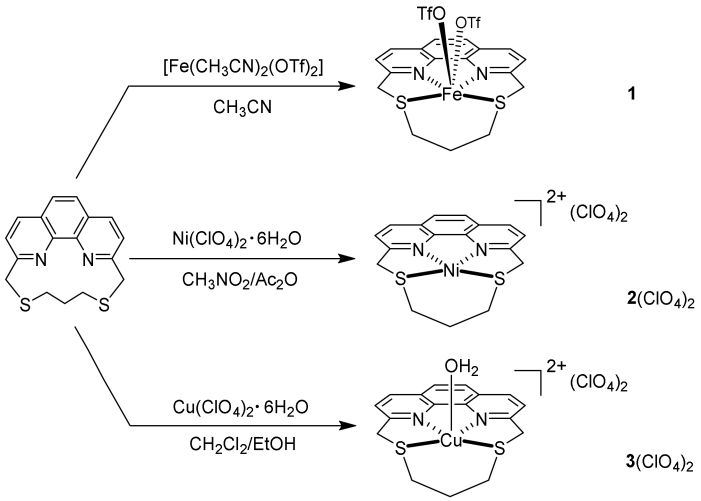

Scheme 3. Synthesis of [13]ane(phenN_2)S_2-containing complexes **1**, **2**$(ClO_4)_2$ and **3**$(ClO_4)_2$.

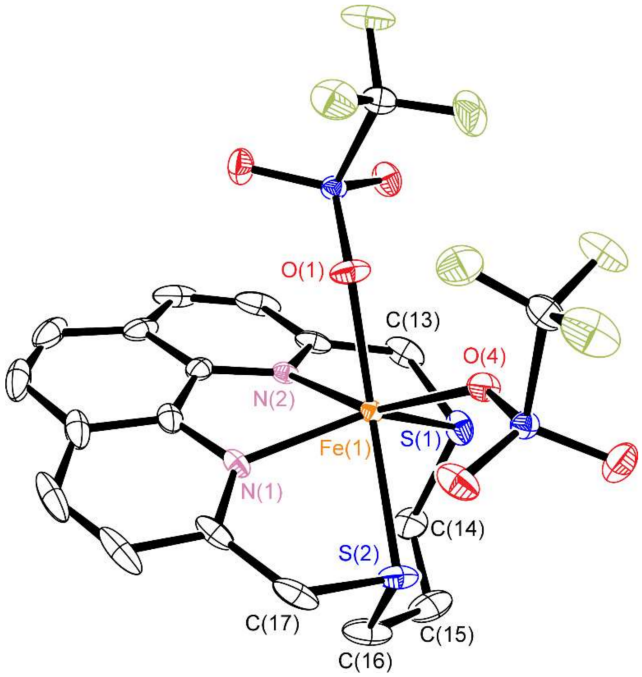

Figure 3. Perspective view of **1** as represented by 30% probability ellipsoids (hydrogen atoms on [13]ane(phenN_2)S_2 are omitted for clarity). Selected bond lengths (Å) and angles (°): Fe(1)-N(1), 2.156(2); Fe(1)-N(2), 2.209(2); Fe(1)-S(1), 2.486(1); Fe(1)-S(2), 2.531(1); Fe(1)-O(1), 2.134(2); Fe(1)-O(4), 2.126(2); N(1)-Fe(1)-N(2), 72.3(1); N(2)-Fe(1)-S(1), 74.5(1); S(1)-Fe(1)-S(2), 92.10(3); N(1)-Fe(1)-S(2), 75.4(1); O(1)-Fe(1)-N(1), 98.8(1); O(1)-Fe(1)-N(2), 81.9(1); O(4)-Fe(1)-S(1), 97.7(1); O(4)-Fe(1)-S(2), 82.6(1).

In high-spin (S = 2) Fe complex **1**, the [13]ane(phenN_2)S_2 acts as a tetradentate ligand, with two N and S atoms coordinating to the Fe center (Figure 3). Meanwhile, the Fe center is coordinated with two O-bound OTf. The coordination of OTf to the Fe center in solution was revealed by ^{19}F-NMR study, with the observation of a single peak at −72.05 ppm indicating the coordinating nature of OTf [55–57]. The coordination geometry of **1** is best described as trigonal prismatic rather than octahedral. As depicted in Figure 4, the angles formed by the lateral faces f_1 and f_2 (61.5°), f_2 and f_3 (59.1°), f_3 and f_1 (60.5°) are all close to 60°, and the angle between the two triangular basal planes of the trigonal prism is small (7.9°), indicating that these basal planes are nearly parallel to each other. The distortion from a perfect trigonal prismatic geometry is characterized by the average twist angle of 14.9°. Meanwhile, the Fe-N (2.156(2)-2.209(2) Å) and Fe-S (2.486(1)-2.531(1) Å) bond distances are

consistent with those of high-spin Fe(II) species bearing diimine moiety [58] and thioether linker [59]. The Fe-O bond distances (2.126(2)-2.134(2) Å) of **1** are typical of known high-spin Fe(II) complexes bearing coordinated OTf (2.025-2.211 Å) [60–62].

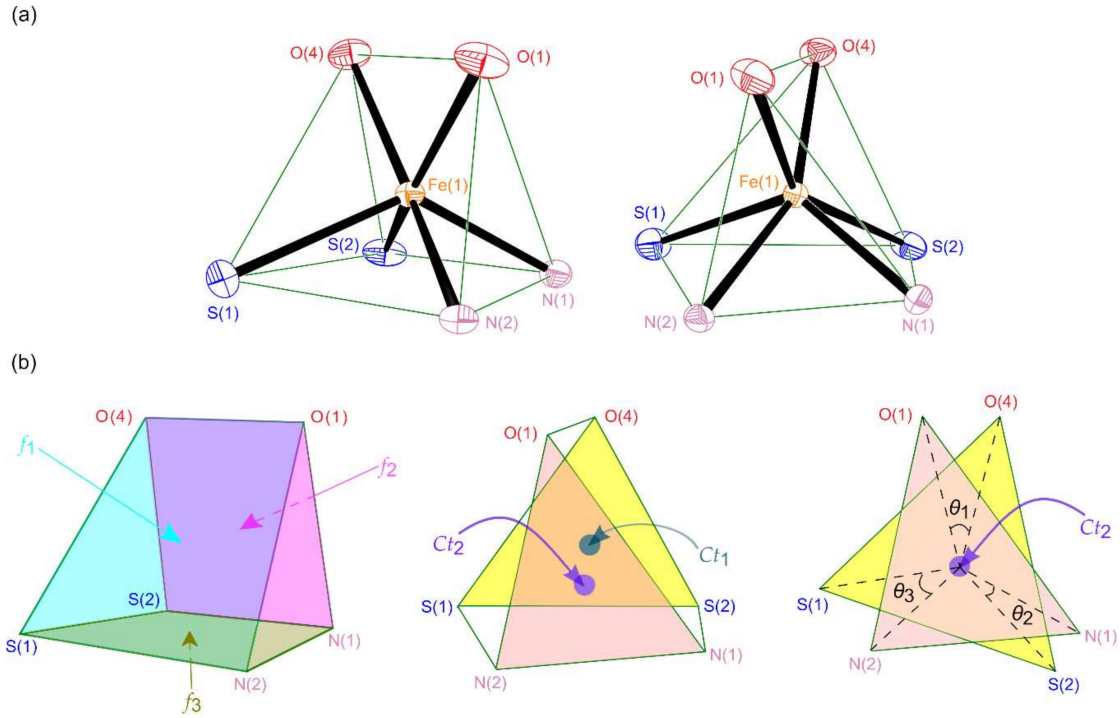

Figure 4. (**a**) Two different views of the coordination environment surrounding the Fe center of **1** and (**b**) illustrations of the three lateral faces (f_1–f_3), centroids (Ct_1 and Ct_2) and twist angles (θ_1–θ_3) of the two triangular basal planes on the twisted trigonal prism.

In high-spin (S = 1) **2**$(ClO_4)_2$, the Ni atom adopts a square planar geometry with the N and S atoms of [13]ane(phenN_2)S_2 occupying the equatorial position (Figure 5). The Ni atom only lies above the mean plane constructed by the four coordinating atoms of [13]ane(phenN_2)S_2 by 0.073 Å, and the geometry index τ [63,64] calculated for this complex is 0.11 (cf. $\tau \approx 0$ and $\tau \approx 1$ for square planar and tetrahedral geometry, respectively, in four-coordinated compounds). In comparison with $[Ni([15]ane(phenN_2)S_3(CH_3CN)]^{2+}$ where the Ni atom adopts a distorted octahedral geometry [46], the Ni-N and Ni-S bond distances in **2**$(ClO_4)_2$ (1.849(2)-1.855(2) Å for Ni-N, 2.155(1)-2.156(1) Å for Ni-S) are shorter than those in $[Ni([15]ane(phenN_2)S_3(CH_3CN)]^{2+}$ (2.013(2)–2.025(2) Å for Ni-N, 2.434(1)-2.444(1) Å for Ni-S). These observations are probably originated from the restricted flexibility of the shorter aliphatic linker in [13]ane(phenN_2)S_2.

In **3**$(ClO_4)_2$, the Cu atom adopts a square pyramidal geometry (τ = 0.02; cf. $\tau \approx 0$ and $\tau \approx 1$ for square pyramidal and trigonal bipyramidal geometry, respectively, in five-coordinated compounds), with the N and S atoms of [13]ane(phenN_2)S_2 occupying the equatorial position, and the O atom of H_2O in the axial position (Figure 6). The Cu atom is found to be located above the mean plane constructed by the four coordinating atoms of [13]ane(phenN_2)S_2 by 0.444 Å. The Cu-N bond distances of **3**$(ClO_4)_2$ (1.950(3)-1.963(3) Å) are comparable to that in $[Cu([15]ane(phenN_2)S_2)(ClO_4)]^+$ (1.956(5) Å) [47]. On the other hand, the Cu-S bond distances in **3**$(ClO_4)_2$ (2.292(1)-2.296(1) Å) are shorter than those in $[Cu([15]ane(phenN_2)S_2)(ClO_4)]^+$ (2.347(2) Å). This again reflects the restricted flexibility of the shorter aliphatic linker in [13]ane(phenN_2)S_2.

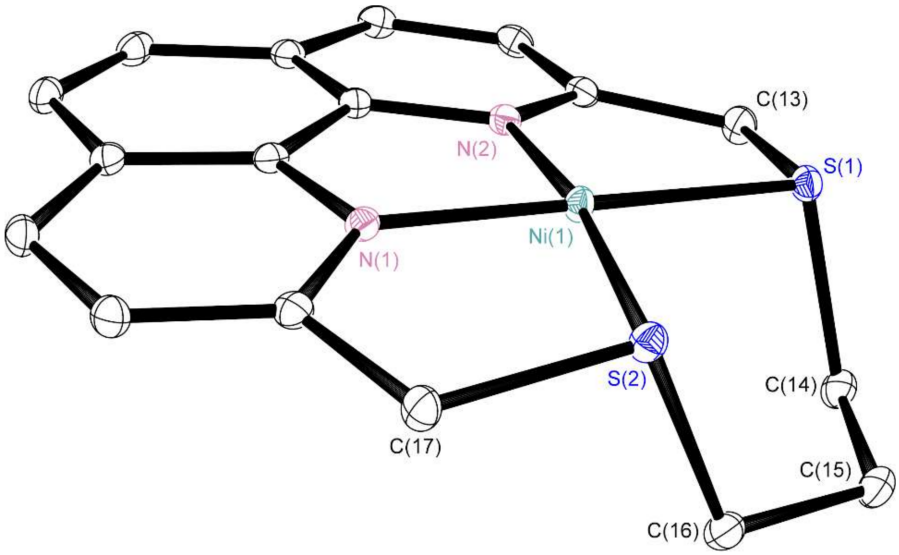

Figure 5. Perspective view of **2** as represented by 30% probability ellipsoids (hydrogen atoms on [13]ane(phenN_2)S_2 are omitted for clarity). Selected bond lengths (Å) and angles (°): Ni(1)-N(1), 1.849(2); Ni(1)-N(2), 1.855(2); Ni(1)-S(1), 2.155(1); Ni(1)-S(2), 2.156(1); N(1)-Ni(1)-N(2), 85.3(1); N(2)-Ni(1)-S(1), 87.5(1); S(1)-Ni(1)-S(2), 99.10(2); S(2)-Ni(1)-N(1), 87.8(1).

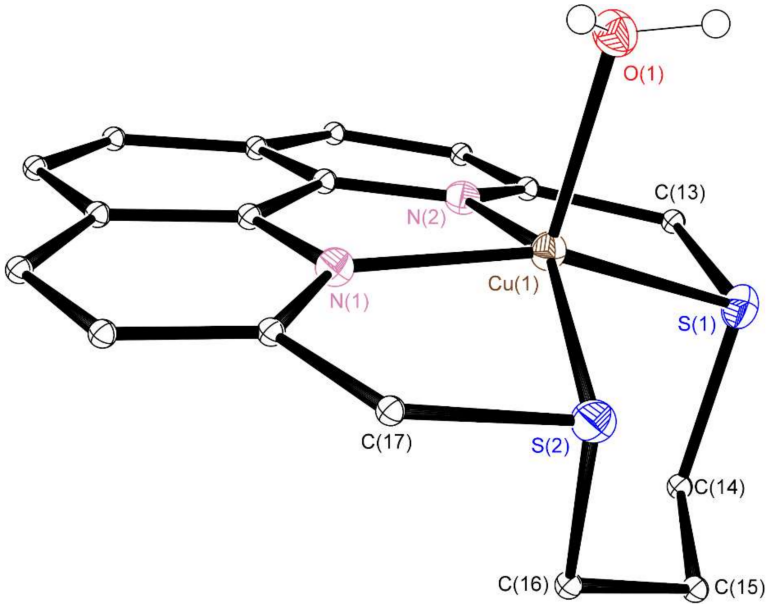

Figure 6. Perspective view of **3** as represented by 30% probability ellipsoids (hydrogen atoms on [13]ane(phenN_2)S_2 are omitted for clarity). Only one of the independent cations in [**3**$(ClO_4)_2]_2$ is depicted. Selected bond lengths (Å) and angles (°) are listed in the order of Cu(1) moiety and then Cu(2) moiety: Cu(1)-N(1), 1.963(3), 1.950(3); Cu(1)−N(2), 1.959(3), 1.955(3); Cu(1)-S(1), 2.293(1), 2.293(1); Cu(1)-S(2), 2.292(1), 2.296(1); Cu(1)-O(1), 2.160(3), 2.165(3); N(1)-Cu(1)-N(2), 81.6(1), 82.1(2); N(2)-Cu(1)-S(1), 84.5(1), 84.4(1); S(1)-Cu(1)-S(2), 99.72(4), 100.51(4); S(2)-Cu(1)-N(1), 84.1(1), 84.2(1).

3. Materials and Methods

3.1. General Procedures

All reactions were performed under an argon atmosphere using standard Schlenk techniques unless otherwise stated. All reagents were used as received, and solvents for reactions were purified by a PureSolv MD5 solvent purification (Amesbury, MA, USA) system.

The 2,9-dicarbaldehyde-1,10-phenanthroline [50,52], 2,9-bis(hydroxymethyl)-1,10-phenanthroline [51], 2,9-bis(chloromethyl)-1,10-phenanthroline [48,49] and $Fe(CH_3CN)_2(OTf)_2$ [65], were prepared in accordance with the literature methods. ^{1}H, ^{13}C{^{1}H}, ^{1}H-^{1}H COSY, ^{1}H-^{1}H-ROESY, ^{1}H–^{13}C-HSQC and ^{1}H-^{13}C-HMBC-NMR spectra were recorded on a Bruker 600 AVANCE III FT-NMR spectrometer (Billerica, MA, USA). Peak positions were calibrated with solvent residue peaks as internal standard. Labeling scheme for H and C atoms in the NMR assignments is shown in Scheme 4. Electrospray mass spectrometry was performed on a PE-SCIEX API 3200 triple quadrupole mass spectrometer (Tokyo, Japan). Elemental analyses were done on an Elementar Vario Micro Cube carbon-hydrogen-nitrogen elemental microanalyzer (Okehampton, UK). UV-visible spectra were recorded on a Shimadzu UV-1800 spectrophotometer (San Francisco, CA, USA). Neocuproine (98%), nickel(II) perchlorate hexahydrate ($Ni(ClO_4)_2{\cdot}6H_2O$) and copper(II) perchlorate hexahydrate ($Cu(ClO_4)_2{\cdot}6H_2O$) were purchased from J&K Scientific Ltd (Hong Kong). Iron(II) chloride ($FeCl_2$, anhydrous, 98%) and trimethylsilyl trifluoromethanesulphonate ($(CH_3)_3SiOTf$, 98%) were purchased from Fluorochem Ltd. (Derbyshire, UK)

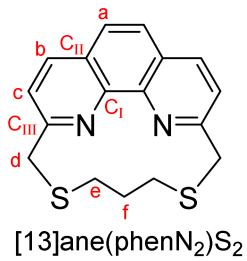

[13]ane(phenN_2)S_2

Scheme 4. Labeling scheme for H and C atoms in [13]ane(phenN_2)S_2.

3.2. Solution Magnetic Susceptibility Measurements

The solution state molar magnetic susceptibility (χ_m) of **1**, **2**$(ClO_4)_2$ and **3**$(ClO_4)_2$ was measured according to the Evans method [53,54]. This involves the placement of a coaxial insert containing sample solution (0.010 M) into a standard 5 mm NMR tube containing only solvent. CD_3CN containing one drop of benzene as internal reference was used as the solvent throughout. Based on the chemical shift difference of the benzene internal reference between inner and outer tubes, values of molar magnetic susceptibility (χ_m) and magnetic moment (μ_{eff}) were calculated using the equations shown below [66,67]:

$$\chi_m = (3{\cdot}\Delta f)/(1000{\cdot}f{\cdot}c) \quad (1)$$

$$\mu_{eff} = 798\sqrt{T{\cdot}\chi_m} \quad (2)$$

where χ_m = molar magnetic susceptibility of the sample (m^3 mol^{-1}); $\triangle$f = difference of the chemical shift (Hz) between the internal references of inner and outer tubes; f = operating frequency of the NMR spectrometer (Hz); c = concentration of the metal complex (mol dm^{-3}); T = probe temperature of the measurement (K).

3.3. Geometry Index

The geometry index (τ) is a parameter ranging from 0 to 1 to describe the geometry of the coordination center in four- and five-coordinated compounds.

For four-coordinated compounds, the τ is used to distinguish whether the coordination geometry of the metal center is square planar ($\tau \approx 0$) or tetrahedral ($\tau \approx 1$) [64]. The formula is shown below:

$$\tau = (\beta - \alpha)/(360^\circ - \theta) + (180^\circ - \beta)/(180^\circ - \theta) \approx -0.00399\alpha - 0.01019\beta + 2.55 \quad (3)$$

where α and β are the two largest valence angles of the coordination center ($\beta > \alpha$) and $\theta = \cos^{-1}(-1/3) \approx 109.5^\circ$ is a tetrahedral angle.

For **2**$(ClO_4)_2$, α(N(2)-Ni(1)-S(2)) = 171.9° and β(N(1)-Ni(1)-S(1)) = 172.0°.

For five-coordinated compounds, the τ is used to distinguish whether the coordination geometry of the metal center is square pyramidal (τ ≈ 0) or trigonal bipyramidal (τ ≈ 1) [63]. The formula is shown below:

$$\tau = (\beta - \alpha)/60^\circ \approx -0.01667\alpha + 0.01667\beta \quad (4)$$

where α and β are the two largest valence angles of the coordination center (β > α).

For **3**$(ClO_4)_2$, α(N(1)-Cu(1)-S(1)) = 154.0° and β(N(2)-Cu(1)-S(2)) = 155.0°.

3.4. Synthesis of ([13]ane(phenN_2)S_2) and [13]ane(phenN_2)S_2-containing Fe(II), Ni(II), Cu(II) complexes

Synthesis of 2,9-dicarbaldehyde-1,10-phenanthroline. The ligand was synthesized from a modified literature procedure [52]: To a solution of selenium oxide (2.26 g, 20.41 mmol) in deionized water (5 mL) and 1,4-dioxane (70 mL), 2,9-dimethyl-1,10-phenanthroline (2.00 g, 9.60 mmol) in 1,4-dioxane (20 mL) was added in a dropwise manner. The reaction mixture was refluxed for 0.5 h, during which the color of the reaction mixture changed from yellow to reddish brown with black deposits. Upon cooling to room temperature, the brown solids were collected by suction filtration and washed with Et_2O (10 mL × 3). These solids were further purified by recrystallization with warm $CHCl_3$ and allowed to cool and stand overnight. Yellowish orange solids were collected by suction filtration and washed with Et_2O (10 mL × 3) to give 2,9-dicarbaldehyde-1,10-phenanthroline. ^{1}H-NMR signals are consistent with that of the literature reported [50]. Yield: 1.95 g, 86%.

Synthesis of 2,9-bis(hydroxymethyl)-1,10-phenanthroline. The ligand was synthesized from a modified literature procedure [51]: To a solution of 2,9-dicarbaldehyde-1,10-phenanthroline (1.60 g, 6.77 mmol) in absolute EtOH (120 mL), anhydrous $NaBH_4$ (1.02 g, 27.09 mmol) was added. The reaction mixture was refluxed under argon for 1.5 h, during which the color of the reaction mixture changed from yellow to brown. Upon cooling to room temperature, the reaction mixture was removed by reduced pressure. The aqueous layer was extracted with EtOAc (50 mL × 2). The organic phases were combined, washed with brine (50 mL × 2), dried over anhydrous $MgSO_4$, and concentrated to give 2,9-bis(hydroxymethyl)-1,10-phenanthroline as pale pink solids. ^{1}H-NMR signals are consistent with that of literature reported. Yield: 1.20 g, 74%.

Synthesis of 2,9-bis(chloromethyl)-1,10-phenanthroline. The ligand was synthesized from a modified literature procedure [49]: To a $SOCl_2$ solution (16 mL) at 0 °C, 2,9-bis(hydroxymethyl)-1,10-phenanthroline (1.60 g, 6.66 mmol) was added. The reaction mixture was stirred for 2 h at 0 °C, during which the color of the reaction mixture changed from colorless to yellow. Upon adding *n*-hexane (30 mL) to the reaction mixture, the deep yellow precipitates were collected, dissolved in $CHCl_3$ and extracted with an aqueous layer containing 5% (*w*/*v*) Na_2CO_3 and 5% (*w*/*v*) $NaHCO_3$ for neutralization. The organic phases were combined, washed with brine (50 mL × 2), dried over anhydrous $MgSO_4$ and concentrated to give 2,9-bis(chloromethyl)-1,10-phenanthroline as yellow solids. ^{1}H-NMR signals are consistent with that of literature reported [48]. Yield: 1.52 g, 82%.

Synthesis of 2,6-dithia[7](2,9)-1,10-phenanthrolinophane ([13]ane(phenN_2)S_2). To a well-stirred suspension of dry Cs_2CO_3 (3.34 g, 10.24 mmol) in anhydrous DMF (224 mL) at 55 °C, a mixture of 1,3-propanedithiol (0.51 mL, 5.12 mmol) and 2,9-bis(chloromethyl)-1,10-phenanthroline (1.43 g, 5.12 mmol) in anhydrous DMF (112 mL) was added under argon for 42 h at a rate of 2.67 mL/min, during which the color of the reaction mixture changed from colorless to pale yellow suspension. Upon cooling to room temperature over a period of 24 h, the reaction mixture was removed by vacuum distillation. After dissolving the residue in CH_2Cl_2, the pale orange suspension was filtered to remove Cs_2CO_3. The filtrate was concentrated to give a red oil. The [13]ane(phenN_2)S_2 was obtained as white solids after silica gel column chromatography (silica gel, gradual elution with CH_2Cl_2/EtOAc (8:2, *v*/*v*); R_f value = 0.70 (silica gel TLC; CH_2Cl_2/EtOAc (8:2, *v*/*v*))). Recrystallization by slow diffusion of Et_2O solution into a CH_2Cl_2 solution of the white solids gave analytically pure [13]ane(phenN_2)S_2 as white crystals. Yield:

0.45 g, 30%. Anal. Calcd. for $C_{17}H_{16}N_2S_2$: C, 65.35; H, 5.16; N, 8.97. Found: C, 65.38; H, 5.18; N, 8.99. ESI-MS found (calcd.): *m*/*z* 313.30 (313.46) $[C_{17}H_{16}N_2S_2 + H]^+$. ^{1}H-NMR (600 MHz, $CDCl_3$): δ 2.83–2.98 (m, 2H, H_f), 3.11–3.22 (m, 4H, H_e), 4.12–4.29 (m, 4H, H_d), 7.43 (d, J = 6.0 Hz, 2H, H_b), 7.73 (s, 2H, H_a), 8.14 (d, J = 6.0 Hz, 2H, H_c). ^{13}C-NMR (150 MHz, $CDCl_3$): δ 34.57 (C_f), 36.72 (C_e), 41.81 (C_d), 121.71 (C_b), 125.73 (C_a), 127.37 (C_{II}), 136.35 (C_c), 146.07 (C_I), 160.79 (C_{III}).

Synthesis of [Fe(CH$_3$CN)$_2$(OTf)$_2$]. The metal precursor was synthesized from a modified literature procedure [65]: To a solution of $FeCl_2$ (0.50 g, 3.94 mmol) in anhydrous CH_3CN (20 mL), $(CH_3)_3SiOTf$ (4 mL in 10 mL anhydrous CH_3CN, 22.10 mmol) was added in a dropwise manner. The reaction mixture was stirred under argon for 16 h, during which the color of the reaction mixture changed from pale yellow to colorless. The colorless solution was concentrated to about 5 mL by reduced pressure, and then added to Et_2O (150 mL) to give white precipitates. The solids were collected by suction filtration, washed with Et_2O (10 mL × 3) and dried by reduced pressure to give $[Fe(CH_3CN)_2(OTf)_2]$. Yield: 1.20 g, 70%.

Synthesis of ***1****.* A mixture of $[Fe(CH_3CN)_2(OTf)_2]$ (0.40 g, 0.91 mmol) and [13]ane(phenN_2)S_2 (0.28 g, 0.91 mmol) was stirred in CH_3CN (30 mL) under argon for 16 h, during which the color of the reaction mixture changed from red to deep red with pale yellow precipitates. Upon filtration for removal of these precipitates, the supernatant was collected and concentrated to give deep red precipitates. The solids were collected by suction filtration and washed with Et_2O (10 mL × 3). Recrystallization by slow diffusion of Et_2O solution into a CH_3CN solution of the deep red solids under argon gave analytically pure **1** as orange crystals. Yield: 0.43 g, 71%. Anal. Calcd. for $C_{19}H_{16}N_2S_4FeF_6O_6$: C, 34.24; H, 2.42; N, 4.20. Found: C, 34.28; H, 2.44; N, 4.21. ^{19}F-NMR (400 MHz, CD_3CN): δ −72.05. ESI-MS found (calcd.): *m*/*z* 517.30 (517.38) $[C_{18}H_{16}N_2S_3FeF_3O_3]^+$. Evans NMR at 298 K: μ_{eff} = 4.98 μ_B.

Synthesis of ***2****(ClO$_4$)$_2$.* To a solution of $Ni(ClO_4)_2{\cdot}6H_2O$ (0.04 g, 0.10 mmol) in nitromethane (15 mL) and acetic anhydride (0.62 mL), [13]ane(phenN_2)S_2 (0.03 g, 0.10 mmol) was added. The reaction mixture was stirred under argon for 2 h, during which the color of the reaction mixture changed from pale green to yellow. The reaction mixture was concentrated to about 5 mL by reduced pressure and then added to Et_2O (150 mL) to give orange precipitates. The solids were collected by suction filtration, washed with deionized water (5 mL × 2), cold EtOH (5 mL × 2), and finally Et_2O (10 mL × 3). Recrystallization by slow diffusion of Et_2O into a CH_3CN solution of the orange precipitates gave analytically pure **2**$(ClO_4)_2$ as brown crystals. Yield: 0.05 g, 80%. Anal. Calcd. for $C_{17}H_{16}N_2S_2NiCl_2O_8$: C, 35.82; H, 2.83; N, 4.91. Found: C, 35.85; H, 2.86; N, 4.93. ESI-MS found (calcd.): *m*/*z* 470.30 (470.60) $[C_{17}H_{16}N_2S_2NiClO_4]^+$. Evans NMR at 298 K: μ_{eff} = 2.77 μ_B.

Synthesis of ***3****(ClO$_4$)$_2$.* To a solution of a mixture of [13]ane(phenN_2)S_2 (0.03 g, 0.10 mmol) in EtOH/CH_2Cl_2 (10 mL, 2:1 (*v*/*v*)), $Cu(ClO_4)_2{\cdot}6H_2O$ (0.89 g, 2.40 mmol) in EtOH (5 mL) was added. The reaction mixture was stirred under argon for 4 h, during which the color of the reaction mixture changed from pale blue to pale purple with bluish green precipitates. The solids were collected by suction filtration, washed with cold EtOH (5 mL × 2), and finally Et_2O (10 mL × 3). Recrystallization by slow diffusion of Et_2O into a CH_3CN solution of the bluish green precipitates gave analytically pure **3**$(ClO_4)_2$ as purple crystals. Yield: 1.00 g, 70%. Anal. Calcd. for $C_{17}H_{18}N_2S_2CuCl_2O_9$: C, 34.44; H, 3.06; N, 4.72. Found: C, 34.48; H, 3.08; N, 4.76. ESI-MS found (calcd.): *m*/*z* 475.30 (475.45) $[C_{17}H_{16}N_2S_2CuClO_4]^+$. Evans NMR at 298 K: μ_{eff} = 1.69 μ_B.

3.5. X-ray Crstayllographic Data

CCDC 1994366–1994369 contain the supplementary crystallographic data for this paper. These data can be obtained free of charge via http://www.ccdc.cam.ac.uk/conts/retrieving.html (or from the CCDC, 12 Union Road, Cambridge CB2 1EZ, UK; Fax: +44 1223 336033; E-mail: deposit@ccdc.cam.ac.uk).

Crystal Data for [13]ane(phenN_2)S_2 ($C_{17}H_{16}N_2S_2$; M = 312.44 g/mol): triclinic, space group P-1 (no. 2), a = 8.7121(4) Å, b = 10.2500(6) Å, c = 10.4864(5) Å, α = 62.718(2)°, β = 68.073(2)°, γ = 70.672(2)°,

V = 757.41(7) Å^3, Z = 2, T = 212.99 K, μ(MoKα) = 0.346 mm^{-1}, *Dcalc* = 1.370 g/cm^3, 9505 reflections measured (4.558° ≤ 2Θ ≤ 52.754°), 3087 unique (R_{int} = 0.0502, R_{sigma} = 0.0514) which were used in all calculations. The final R_1 was 0.0393 (I > 2σ(I)) and wR_2 was 0.0973 (all data). (CCDC 1994366)

Crystal Data for **1** ($C_{19}H_{16}F_6O_6S_4N_2Fe$; M = 666.43 g/mol): monoclinic, space group C2/c (no. 15), a = 28.3742(8) Å, b = 9.9821(3) Å, c = 18.6161(5) Å, β = 112.3340(10)°, V = 4877.2(2) Å^3, Z = 8, T = 172.98 K, μ(MoKα) = 1.048 mm^{-1}, *Dcalc* = 1.815 g/cm^3, 29,372 reflections measured (4.366° ≤ 2Θ ≤ 52.764°), 4989 unique (R_{int} = 0.0523, R_{sigma} = 0.0336) which were used in all calculations. The final R_1 was 0.0367 (I > 2σ(I)) and wR_2 was 0.0898 (all data). (CCDC 1994367)

Crystal Data for **2**$(ClO_4)_2$ ($C_{17}H_{16}N_2O_8S_2Cl_2Ni$; M = 570.05 g/mol): triclinic, space group P-1 (no. 2), a = 8.8218(7) Å, b = 10.0103(8) Å, c = 12.7982(9) Å, α = 108.789(7)°, β = 106.996(7)°, γ = 92.621(6)°, V = 1010.95(13) Å^3, Z = 2, T = 293(2) K, μ(CuKα) = 6.231 mm^{-1}, *Dcalc* = 1.873 g/cm^3, 6468 reflections measured (7.72° ≤ 2Θ ≤ 134.98°), 3576 unique (R_{int} = 0.0202, R_{sigma} = 0.0256) which were used in all calculations. The final R_1 was 0.0295 (I > 2σ(I)) and wR_2 was 0.0810 (all data). (CCDC 1994368)

Crystal Data for **3**$(ClO_4)_2$ ($C_{17}H_{18}N_2O_9S_2Cl_2Cu$; M = 592.89 g/mol): monoclinic, space group $P2_1/c$ (no. 14), a = 26.9718(6) Å, b = 11.0279(3) Å, c = 14.7341(3) Å, β = 99.779(2)°, V = 4318.87(18) Å^3, Z = 8, T = 293(2) K, μ(MoKα) = 1.508 mm^{-1}, *Dcalc* = 1.824 g/cm^3, 20,460 reflections measured (6.62° ≤ 2Θ ≤ 53°), 8925 unique (R_{int} = 0.0213, R_{sigma} = 0.0291) which were used in all calculations. The final R_1 was 0.0487 (I >2σ(I)) and wR_2 was 0.1291 (all data). (CCDC 1994369)

3.6. Computational Methodology

The structures and relative energies of Conformers **I**–**III** were calculated by density functional theory (DFT) calculations using the ORCA software package (version 4.1.1, Max-Planck-Institut für Chemische Energiekonversion, Mülheim an der Ruhr, North Rhine-Westphalia, Germany) [68]. All the calculated structures were optimized in the gas phase at the BP86/def2-SVP level with the Grimme's DFTD3 method to account for the dispersion effects, and the Resolution of Identity (RI) approximation to speed up the calculations. Tight self-consistent field (SCF) convergence criteria were used throughout. The optimized conformers were confirmed to be local minima via frequency calculations (no negative frequency).

4. Conclusions

A new tetradentate mixed aza-thioether macrocyclic ligand 2,6-dithia[7](2,9)-1,10-phenanthrolinophane ([13]ane(phenN_2)S_2) was successfully prepared. Three low-valent first-row transition metal complexes supported by [13]ane(phenN_2)S_2, namely [Fe([13]ane(phenN_2)S_2)$(OTf)_2$], [Ni([13]ane(phenN_2)S_2)]$(ClO_4)_2$ and [Cu([13]ane(phenN_2)S_2)(OH_2)]$(ClO_4)_2$, were synthesized from reactions between corresponding transition metal precursors and [13]ane(phenN_2)S_2 under mild reaction conditions. The X-ray structures of the metal complexes revealed that [13]ane(phenN_2)S_2 acts as a tetradentate ligand by coordinating to the metal centers via donor atoms N and S. The success of preparing these macrocyclic complexes undeniably opens new opportunities for further reactivity studies and possible biological applications.

Supplementary Materials: The following are available online, Table S1–S3: Cartesian coordinates of calculated structures of Conformers **I**–**III**. Figure S1: UV-visible absorption spectra of **1**, **2**$(ClO_4)_2$ and **3**$(ClO_4)_2$ in CH_3CN at 298 K, Figure S2: ^{1}H-NMR spectrum of [13]ane(phenN_2)S_2, Figure S3: $^{13}C\{^1H\}$-NMR spectrum of [13]ane(phenN_2)S_2, Figure S4: ^{1}H-^{1}H COSY of [13]ane(phenN_2)S_2, Figure S5: ^{1}H-^{1}H ROESY of [13]ane(phenN_2)S_2, Figure S6: ^{1}H-^{13}C HSQC of [13]ane(phenN_2)S_2, Figure S7: ^{1}H-^{13}C HMBC of [13]ane(phenN_2)S_2.

Author Contributions: Conceptualization, S.-W.N., S.-C.C., C.-Y.W.; investigation, S.-W.N., S.-C.C., C.-F.Y., S.-M.Y.; writing—original draft preparation, S.-W.N., S.-C.C.; writing—review and editing, S.-W.N., C.-Y.W.; supervision, C.-Y.W.; funding acquisition, C.-Y.W. All authors have read and agreed to the published version of the manuscript.

Funding: The work described in this paper was supported by the Research Grants Council of Hong Kong SAR (CityU 11207117 and T42-103/16-N) and City University of Hong Kong (7005096, 7005257, 9680206).

Conflicts of Interest: The authors declare no conflict of interest.

References

1. Hubin, T.J. Synthesis and coordination chemistry of topologically constrained azamacrocycles. *Coord. Chem. Rev.* **2003**, *241*, 27–46. [CrossRef]
2. MacKay, B.A.; Fryzuk, M.D. Dinitrogen Coordination Chemistry: On the Biomimetic Borderlands. *Chem. Rev.* **2004**, *104*, 385–401. [CrossRef]
3. Friedle, S.; Reisner, E.; Lippard, S.J. Current challenges of modeling diiron enzyme active sites for dioxygen activation by biomimetic synthetic complexes. *Chem. Soc. Rev.* **2010**, *39*, 2768–2779. [CrossRef]
4. Marchetti, L.; Levine, M. Biomimetic Catalysis. *ACS Catal.* **2011**, *1*, 1090–1118. [CrossRef]
5. Zhao, M.; Wang, H.-B.; Ji, L.-N.; Mao, Z.-W. Insights into metalloenzyme microenvironments: Biomimetic metal complexes with a functional second coordination sphere. *Chem. Soc. Rev.* **2013**, *42*, 8360–8375. [CrossRef]
6. Ray, K.; Pfaff, F.F.; Wang, B.; Nam, W. Status of Reactive Non-Heme Metal-Oxygen Intermediates in Chemical and Enzymatic Reactions. *J. Am. Chem. Soc.* **2014**, *136*, 13942–13958. [CrossRef]
7. Rebilly, J.-N.; Colasson, B.; Bistri, O.; Over, D.; Reinaud, O. Biomimetic cavity-based metal complexes. *Chem. Soc. Rev.* **2015**, *44*, 467–489. [CrossRef]
8. Joshi, T.; Graham, B.; Spiccia, L. Macrocyclic Metal Complexes for Metalloenzyme Mimicry and Sensor Development. *Acc. Chem. Res.* **2015**, *48*, 2366–2379. [CrossRef]
9. Sahu, S.; Goldberg, D.P. Activation of Dioxygen by Iron and Manganese Complexes: A Heme and Nonheme Perspective. *J. Am. Chem. Soc.* **2016**, *138*, 11410–11428. [CrossRef]
10. Engelmann, X.; Monte-Pérez, I.; Ray, K. Oxidation Reactions with Bioinspired Mononuclear Non-Heme Metal-Oxo Complexes. *Angew. Chem. Int. Ed.* **2016**, *55*, 7632–7649. [CrossRef]
11. Baglia, R.A.; Zaragoza, J.P.T.; Goldberg, D.P. Biomimetic Reactivity of Oxygen-Derived Manganese and Iron Porphyrinoid Complexes. *Chem. Rev.* **2017**, *117*, 13320–13352. [CrossRef]
12. Joshi, T.; Kubeil, M.; Nsubuga, A.; Singh, G.; Gasser, G.; Stephan, H. Harnessing the Coordination Chemistry of 1,4,7-Triazacyclononane for Biomimicry and Radiopharmaceutical Applications. *ChemPlusChem* **2018**, *83*, 554–564. [CrossRef]
13. Sun, W.; Sun, Q. Bioinspired Manganese and Iron Complexes for Enantioselective Oxidation Reactions: Ligand Design, Catalytic Activity, and Beyond. *Acc. Chem. Res.* **2019**, *52*, 2370–2381. [CrossRef]
14. Guo, M.; Corona, T.; Ray, K.; Nam, W. Heme and Nonheme High-Valent Iron and Manganese Oxo Cores in Biological and Abiological Oxidation Reactions. *ACS Cent. Sci.* **2019**, *5*, 13–28. [CrossRef]
15. Dearle, A.E.; Cutler, D.J.; Fraser, H.W.L.; Sanz, S.; Lee, E.; Dey, S.; Diaz-Ortega, I.F.; Nichol, G.S.; Nojiri, H.; Evangelisti, M.; et al. An $[Fe^{III}_{34}]$ Molecular Metal Oxide. *Angew. Chem. Int. Ed.* **2019**, *58*, 16903–16906. [CrossRef]
16. Wong, C.-Y.; Lai, L.-M.; Lam, C.-Y.; Zhu, N. Ruthenium Carbene and Allenylidene Complexes Supported by the Tertiary Amine-Aromatic Diimine Ligand Set: Structural, Spectroscopic, and Theoretical Studies. *Organometallics* **2008**, *27*, 5806–5814. [CrossRef]
17. Wong, C.-Y.; Lai, L.-M.; Pat, P.-K. Ruthenium Acetylide Complexes Supported by Trithiacyclononane and Aromatic Diimine: Structural, Spectroscopic, and Theoretical Studies. *Organometallics* **2009**, *28*, 5656–5660. [CrossRef]
18. Wong, C.-Y.; Lai, L.-M.; Chan, S.-C.; Tai, L.-H. Photophysical and Theoretical Studies of Ruthenium(II)-Acetylide and -Cyanide Complexes with Aromatic Diimine and Trithiacyclononane. *Organometallics* **2010**, *29*, 6259–6266. [CrossRef]
19. Chung, L.-H.; Wong, C.-Y. Isolation of Ruthenium-Indolizine Complexes: Insight into the Metal-Induced Cycloisomerization of Propargylic Pyridines. *Organometallics* **2013**, *32*, 3583–3586. [CrossRef]
20. Chung, L.-H.; Yeung, C.-F.; Ma, D.-L.; Leung, C.-H.; Wong, C.-Y. Metal-Indolizine Zwitterion Complexes as a New Class of Organometallic Material: A Spectroscopic and Theoretical Investigation. *Organometallics* **2014**, *33*, 3443–3452. [CrossRef]
21. Tsui, W.-K.; Chung, L.-H.; Tsang, W.-H.; Yeung, C.-F.; Chiu, C.-H.; Lo, H.-S.; Wong, C.-Y. Synthesis, Spectroscopic and Theoretical Studies of Ruthenafuran and Osmafuran Prepared by Activation of Ynone in Alcohol. *Organometallics* **2015**, *34*, 1005–1012. [CrossRef]

22. Yeung, C.-F.; Chung, L.-H.; Lo, H.-S.; Chiu, C.-H.; Cai, J.; Wong, C.-Y. Isolation of Ruthenium-Indoline and -Indole Zwitterion Complexes: Insight into the Metal-Induced Cyclization of Aniline-Tethered Alkynes and Strategy to Lower the Activation Barrier of Metal-Vinylidene Formation. *Organometallics* **2015**, *34*, 1963–1968. [CrossRef]
23. Ng, S.-W.; Chung, L.-H.; Yeung, C.-F.; Lo, H.-S.; Shek, H.-L.; Kang, T.-S.; Leung, C.-H.; Ma, D.-L.; Wong, C.-Y. Metalated Chromene and Chromone Complexes: pH Switchable Metal-Carbon Bonding Interaction, Photo-triggerable Chromone Delivery Application, and Antioxidative Activity. *Chem. Eur. J.* **2018**, *24*, 1779–1783. [CrossRef]
24. Chung, L.-H.; Ng, S.-W.; Yeung, C.-F.; Shek, H.-L.; Tse, S.-Y.; Lo, H.-S.; Chan, S.-C.; Tse, M.-K.; Yiu, S.-M.; Wong, C.-Y. Ruthenium-indolizinone complexes as a new class of metalated heterocyclic compounds: Insight into unconventional alkyne activation pathways, revelation of unexpected electronic properties and exploration of medicinal application. *Dalton Trans.* **2018**, *47*, 12838–12842. [CrossRef]
25. Chung, L.-H.; Wong, C.-Y. Ruthenium-Induced Alkyne Cycloisomerization: Construction of Metalated Heterocycles, Revelation of Unconventional Reaction Pathways, and Exploration of Functional Applications. *Chem. Eur. J.* **2019**, *25*, 2889–2897. [CrossRef]
26. Yeung, C.-F.; Chung, L.-H.; Ng, S.-W.; Shek, H.-L.; Tse, S.-Y.; Chan, S.-C.; Tse, M.-K.; Yiu, S.-M.; Wong, C.-Y. Phosphonium-Ring-Fused Bicyclic Metallafuran Complexes of Ruthenium and Osmium. *Chem. Eur. J.* **2019**, *25*, 9159–9163. [CrossRef]
27. Chung, L.-H.; Yeung, C.-F.; Shek, H.-L.; Wong, C.-Y. Isolation of a C3-metalated indolizine complex and a phosphonium ring-fused bicyclic metallafuran from the osmium-induced transformation of pyridine-tethered alkynes. *Faraday Discuss.* **2019**, *220*, 196–207. [CrossRef]
28. Aoki, Y.; Bauer, M.; Braun, T.; Cadge, J.A.; Clarke, G.E.; Durand, D.J.; Eisenstein, O.; Gallarati, S.; Greaves, M.; Harvey, J.; et al. Mechanistic insight into organic and industrial transformations: General discussion. *Faraday Discuss.* **2019**, *220*, 282–316. [CrossRef]
29. Ng, S.-W.; Tse, S.-Y.; Yeung, C.-F.; Chung, L.-H.; Tse, M.-K.; Yiu, S.-M.; Wong, C.-Y. Ru(II)- and Os(II)-Induced Cycloisomerization of Phenol-Tethered Alkyne for Functional Chromene and Chromone Complexes. *Organometallics* **2020**, *39*, 1299–1309. [CrossRef]
30. Contu, F.; Demartin, F.; Devillanova, F.A.; Garau, A.; Isaia, F.; Lippolis, V.; Salis, A.; Verani, G. Conformationally locked mixed aza-thioether macrocycles: Synthesis and structures of complexes of Pd^{II}, Pt^{II} and Rh^{III} of 2,5,8-trithia-[9](2,9)-1,10-phenanthrolinophane. *J. Chem. Soc. Dalton Trans.* **1997**, 4401–4405. [CrossRef]
31. Blake, A.J.; Casabò, J.; Devillanova, F.A.; Escriche, L.; Garau, A.; Isaia, F.; Lippolis, V.; Kivekas, R.; Muns, V.; Schröder, M.; et al. Mixed aza–thioether crowns containing the 1,10-phenanthroline sub-unit. Substitution reactions in $[NiL(MeCN)][BF_4]_2$ {L = 2,5,8-trithia[9](2,9)-1,10-phenanthrolinophane}. *J. Chem. Soc. Dalton Trans.* **1999**, 1085–1092. [CrossRef]
32. Shamsipur, M.; Javanbakht, M.; Mousavi, M.F.; Ganjali, M.R.; Lippolis, V.; Garau, A.; Tei, L. Copper(II)-selective membrane electrodes based on some recently synthesized mixed aza-thioether crowns containing a 1,10-phenanthroline sub-unit. *Talanta* **2001**, *55*, 1047–1054. [CrossRef]
33. Arca, M.; Blake, A.J.; Casabò, J.; Demartin, F.; Devillanova, F.A.; Garau, A.; Isaia, F.; Lippolis, V.; Kivekas, R.; Muns, V.; et al. Conformationally locked pentadentate macrocycles containing the 1,10-phenanthroline unit. Synthesis and crystal structure of 5-oxa-2,8-dithia[9](2,9)-1,10-phenanthrolinophane (L) and its coordination properties to Ni^{II}, Pd^{II}, Pt^{II}, Rh^{III} and Ru^{II}. *J. Chem. Soc. Dalton Trans.* **2001**, 1180–1188. [CrossRef]
34. Shamsipur, M.; Javanbakht, M.; Lippolis, V.; Garau, A.; De Filippo, G.; Ganjali, M.R.; Yari, A. Novel Ag^{+} ion-selective electrodes based on two new mixed azathioether crowns containing a 1,10-phenanthroline sub-unit. *Anal. Chim. Acta* **2002**, *462*, 225–234. [CrossRef]
35. Aragoni, M.C.; Arca, M.; Demartin, F.; Devillanova, F.A.; Isaia, F.; Garau, A.; Lippolis, V.; Jalali, F.; Papke, U.; Shamsipur, M.; et al. Fluorometric Chemosensors. Interaction of Toxic Heavy Metal Ions Pb^{II}, Cd^{II}, and Hg^{II} with Novel Mixed-Donor Phenanthroline-Containing Macrocycles: Spectrofluorometric, Conductometric, and Crystallographic Studies. *Inorg. Chem.* **2002**, *41*, 6623–6632. [CrossRef] [PubMed]
36. Shamsipur, M.; Javanbakht, M.; Ganjali, M.R.; Mousavi, M.F.; Lippolis, V.; Garau, A. Mixed Aza-Thioether Crowns Containing a 1,10-Phenanthroline Sub-Unit as Neutral Ionophores for Silver Ion. *Electroanalysis* **2002**, *14*, 1691–1698. [CrossRef]

37. Blake, A.J.; Caçote, M.H.M.; Devillanova, F.A.; Garau, A.; Isaia, F.; Lippolis, V.; Pereira, C.M.; Silva, F.; Tei, L. Coordination Chemistry of 2,5,8-Trithia[9],(2,9)-1,10-phenanthrolinophane (L) toward Rhodium(III) at the Polarised Water/1,2-Dichloroethane Interface—A Possible New Approach to the Problem of Separating Rh^{III} from Chloride Media. *Eur. J. Inorg. Chem.* **2002**, 1816–1822. [CrossRef]
38. Shamsipur, M.; Kazemi, S.Y.; Azimi, G.; Madaeni, S.S.; Lippolis, V.; Garau, A.; Isaia, F. Selective transport of silver ion through a supported liquid membrane using some mixed aza-thioether crowns containing a 1,10-phenanthroline sub-unit as specific ion carriers. *J. Membr. Sc.* **2003**, *215*, 87–93. [CrossRef]
39. De Filippo, G.; Demartin, F.; Garau, A.; Lippolis, V.; Yari, A.; Shokrollahi, A.; Shamsipur, M. Complexes of Ag^{+} with mixed donor phenanthroline-containing macrocycles: Spectrofluorimetric, spectrophotometric, conductometric and potentiometric studies. *Inorg. Chim. Acta* **2005**, *358*, 801–807. [CrossRef]
40. Shamsipur, M.; Hashemi, O.R.; Lippolis, V. A supported liquid membrane system for simultaneous separation of silver(I) and mercury(II) from dilute feed solutions. *J. Membr. Sc.* **2006**, *282*, 322–327. [CrossRef]
41. Ferreira, E.S.; Garau, A.; Lippolis, V.; Pereira, C.M.; Silva, F. Electrochemistry of 2,8-dithia[9],(2,9)-1,10-phenanthrolinophane (L) at the polarized water/1,2-dichloroethane interface: Evaluation of the complexation properties towards transition and *post*-transition metal ions. *J. Electroanal. Chem.* **2006**, *587*, 155–160. [CrossRef]
42. Aragoni, M.C.; Arca, M.; Bencini, A.; Biagini, S.; Blake, A.J.; Caltagirone, C.; Demartin, F.; De Filippo, G.; Devillanova, F.A.; Garau, A.; et al. Interaction of Mixed-Donor Macrocycles Containing the 1,10-Phenanthroline Subunit with Selected Transition and Post-Transition Metal Ions: Metal Ion Recognition in Competitive Liquid-Liquid Solvent Extraction of Cu^{II}, Zn^{II}, Pb^{II}, Cd^{II}, Ag^{I}, and Hg^{II}. *Inorg. Chem.* **2008**, *47*, 8391–8404. [CrossRef] [PubMed]
43. Gulaboski, R.; Ferreira, E.S.; Pereira, C.M.; Cordeiro, M.N.D.S.; Garau, A.; Lippolis, V.; Silva, A.F. Coupling of Cyclic Voltammetry and Electrochemical Impedance Spectroscopy for Probing the Thermodynamics of Facilitated Ion Transfer Reactions Exhibiting Chemical Kinetic Hindrances. *J. Phys. Chem. C* **2008**, *112*, 153–161. [CrossRef]
44. Shamsipur, M.; Hashemi, B.; Dehdashtian, S.; Mohammadi, M.; Gholivand, M.B.; Garau, A.; Lippolis, V. Silver ion imprinted polymer nanobeads based on a aza-thioether crown containing a 1,10-phenanthroline subunit for solid phase extraction and for voltammetric and potentiometric silver sensors. *Anal. Chim. Acta* **2014**, *852*, 223–235. [CrossRef]
45. Casula, A.; Nairi, V.; Fernández-Moreira, V.; Laguna, A.; Lippolis, V.; Garau, A.; Gimeno, M.C. Re(I) derivatives functionalised with thioether crowns containing the 1,10-phenanthroline subunit as a new class of chemosensors. *Dalton Trans.* **2015**, *44*, 18506–18517. [CrossRef]
46. Blake, A.J.; Demartin, F.; Devillanova, F.A.; Garau, A.; Isaia, F.; Lippolis, V.; Schröder, M.; Verani, G. A new class of mixed aza-thioether crown containing a 1,10-phenanthroline sub-unit. *J. Chem. Soc. Dalton Trans.* **1996**, 3705–3712. [CrossRef]
47. Arca, M.; Azimi, G.; Demartin, F.; Devillanova, F.A.; Escriche, L.; Garau, A.; Isaia, F.; Kivekas, R.; Lippolis, V.; Muns, V.; et al. Complexes of Cu^{II} with mixed-donor phenanthroline-containing macrocycles: Analysis of their structural, redox and spectral properties in the context of Type-1 blue copper proteins biomimetic models. *Inorg. Chim. Acta.* **2005**, *358*, 2403–2412. [CrossRef]
48. Newkome, G.R.; Kiefer, G.E.; Puckett, W.E.; Vreeland, T. α-Methyl Functionalization of Electron-Poor Heterocycles: 2,9-Bis(chloromethyl)-1,10-phenanthroline. Synthesis of a [3.3]Cyclophane Containing the 1,10-Phenanthrolino Moiety. *J. Org. Chem.* **1983**, *48*, 5112–5114. [CrossRef]
49. Weijnen, J.G.J.; Engbersen, J.F.J. Catalytic hydrolysis of phosphate esters by metallocomplexes of 1,10-phenanthroline derivatives in micellar solution. *Recl. Trav. Chim. Pays-Bas* **1993**, *112*, 351–357. [CrossRef]
50. De Cian, A.; DeLemos, E.; Mergny, J.-L.; Teulade-Fichou, M.-P.; Monchaud, D. Highly Efficient G-Quadruplex Recognition by Bisquinolinium Compounds. *J. Am. Chem. Soc.* **2007**, *129*, 1856–1857. [CrossRef]
51. Higashi, T.; Inami, K.; Mochizuki, M. Synthesis and DNA-binding Properties of 1,10-Phenanthroline Analogues as Intercalating-Crosslinkers. *J. Heterocyclic Chem.* **2008**, *45*, 1889–1892. [CrossRef]
52. Yang, Y.; Liu, J.; Yang, L.; Li, K.; Zhang, H.; Luo, S.; Rao, L. Probing the difference in covalence by enthalpy measurements: A new heterocyclic N-donor ligand for actinide/lanthanide separation. *Dalton Trans.* **2015**, *44*, 8959–8970. [CrossRef] [PubMed]

53. Evans, D. 400. The Determination of the Paramagnetic Susceptibility of Substances in Solution by Nuclear Magnetic Resonance. *J. Chem. Soc.* **1959**, 2003–2005. [CrossRef]
54. Grant, D.H. Paramagnetic Susceptibility by NMR: The "Solvent Correction" Reexamined. *J. Chem. Educ.* **1995**, *72*, 39–40. [CrossRef]
55. Britovsek, G.J.P.; England, J.; White, A.J.P. Non-heme Iron(II) Complexes Containing Tripodal Tetradentate Nitrogen Ligands and Their Application in Alkane Oxidation Catalysis. *Inorg. Chem.* **2005**, *44*, 8125–8134. [CrossRef]
56. England, J.; Gondhia, R.; Bigorra-Lopez, L.; Petersen, A.R.; White, A.J.P. Towards robust alkane oxidation catalysts: Electronic variations in non-heme iron(II) complexes and their effect in catalytic alkane oxidation. *Dalton Trans.* **2009**, 5319–5334. [CrossRef]
57. Ayad, M.; Klein Gebbink, R.J.M.; Le Mest, Y.; Schollhammer, P.; Le Poul, N.; Pétillon, F.Y.; Mandon, D. Mononuclear iron(II) complexes containing a tripodal and macrocyclic nitrogen ligand: Synthesis, reactivity and application in cyclohexane oxidation catalysis. *Dalton Trans.* **2018**, *47*, 15596–15612. [CrossRef]
58. Ossinger, S.; Naggert, H.; Bill, E.; Näther, C.; Tuczek, F. Electronic Structure, Vibrational Spectra, and Spin-Crossover Properties of Vacuum-Evaporable Iron(II) Bis(dihydrobis(pyrazolyl)borate) Complexes with Diimine Coligands. Origin of Giant Raman Features. *Inorg. Chem.* **2019**, *58*, 12873–12887. [CrossRef]
59. Hughes, D.L.; Jimenez-Tenorio, M.; Leigh, G.J.; Houlton, A.; Silver, J. Iron Complexes with Polythioether Ligands: The Relation of Unusually Large Mössbauer Quadrupole Splittings to Structure. *J. Chem. Soc. Dalton Trans.* **1992**, 2033–2037. [CrossRef]
60. Benhamou, L.; Thibon, A.; Brelot, L.; Lachkar, M.; Mandon, D. Structural bases of oxygen-sensitivity in Fe(II) complexes with tripodal ligands. Steric effects, Lewis acidity and the role of ancillary ligands. *Dalton Trans.* **2012**, *41*, 14369–14380. [CrossRef]
61. Panchbhai, G.; Singh, W.M.; Das, B.; Jane, R.T.; Thapper, A. Mononuclear Iron Complexes with Tetraazadentate Ligands as Water Oxidation Catalysts. *Eur. J. Inorg. Chem* **2016**, 3262–3268. [CrossRef]
62. Li, J.; Molenda, M.A.; Biros, S.M.; Staples, R.J.; Chavez, F.A. Assembly of a mononuclear ferrous site using a bulky aldehyde-imidazole ligand. *Inorg. Chim. Acta* **2017**, *464*, 152–156. [CrossRef] [PubMed]
63. Addison, A.W.; Nageswara Rao, T.; Reedijk, J.; Van Rijn, J.; Verschoor, G.C. Synthesis, Structure, and Spectroscopic Properties of Copper(II) Compounds containing Nitrogen-Sulphur Donor Ligands; the Crystal and Molecular Structure of Aqua[l,7-bis(*N*-methylbenzimidazol-2'-yl)-2,6-dithiaheptane]copper(II) Perchlorate. *J. Chem. Soc. Dalton Trans.* **1984**, 1349–1356. [CrossRef]
64. Okuniewski, A.; Rosiak, D.; Chojnacki, J.; Becker, B. Coordination polymers and molecular structures among complexes of mercury(II) halides with selected 1-benzoylthioureas. *Polyhedron* **2015**, *90*, 47–57. [CrossRef]
65. Chan, S.-C.; Gupta, P.; Engelmann, X.; Ang, Z.Z.; Ganguly, R.; Bill, E.; Ray, K.; Ye, S.; England, J. Observation of Carbodicarbene Ligand Redox Noninnocence in Highly Oxidized Iron Complexes. *Angew. Chem. Int. Ed.* **2018**, *57*, 15717–15722. [CrossRef] [PubMed]
66. Britovsek, G.J.P.; Gibson, V.C.; Spitzmesser, S.K.; Tellmann, K.P.; White, A.J.P.; Williams, D.J. Cationic 2,6-bis(imino)pyridine iron and cobalt complexes: Synthesis, structures, ethylene polymerisation and ethylene/polar monomer co-polymerisation studies. *J. Chem. Soc. Dalton Trans.* **2002**, 1159–1171. [CrossRef]
67. Chan, S.-C.; Ang, Z.Z.; Gupta, P.; Ganguly, R.; Li, Y.; Ye, S.; England, J. Carbodicarbene Ligand Redox Noninnocence in Highly Oxidized Chromium and Cobalt Complexes. *Inorg. Chem.* **2020**, *59*, 4118–4128. [CrossRef]
68. Neese, F. Software update: The ORCA program system, version 4.0. *WIREs Comput. Mol. Sci.* **2018**, *8*, e1327. [CrossRef]

Sample Availability: Samples of the newly prepared compounds are available from the authors.